

Patterns and comparisons of human-induced changes in river flood impacts in cities

Stephanie Clark^{1*}, Ashish Sharma², Scott A. Sisson¹

1: School of Mathematics and Statistics, University of New South Wales, Sydney, Australia

2: School of Civil and Environmental Engineering, University of New South Wales, Sydney, Australia

** corresponding author*

ABSTRACT

1
2
3
4
5
6
7
8
9
10
11
12
13
14

This study investigates patterns of current conditions and anticipated future changes in city-level flood impacts driven by urbanisation and climate change. Global patterns relating urban river flood impacts to socioeconomic development and changing hydrologic conditions are established, and world cities are matched to these patterns. Comparisons are provided between 98 individual cities. We use a novel adaption of the self-organizing map method to establish and present patterns in the nonlinearly-related environmental and social variables. Output maps of prevalent patterns compare baseline and changing trends of city-specific exposures of population and property to river flooding, revealing relationships between the cities based on their relative map placements. Cities experiencing high (or low) baseline flood impacts on population and/or property that are expected to improve (or worsen), as a result of anticipated climate change and development, are identified and compared. This paper condenses and conveys large amounts of information through visual communication to accelerate the understanding of relationships between local urban conditions and global processes, and to potentially motivate knowledge transfer between decision makers facing similar circumstances.

Keywords: urban hydrology; self-organizing maps; SPATIOTEMPORAL patterns; clustering; city-scale; neural networks; Anthropocene

1 INTRODUCTION

Through urban development and climate change, humans are progressively generating (and being on the receiving end of) increased hydrologic impacts, with these anthropogenically induced changes becoming particularly evident in cities (Revi et al., 2014, Mills 2007, Kreimer et al., 2003; Willems et al., 2012). With high densities of urban populations, infrastructure, property and industry, cities are both substantial drivers and receivers of environmental impacts. River flooding, the environmental event affecting more people than any other natural hazard (Doocy et al., 2013; Desai et al., 2015; Sofia et al., 2016), currently poses a threat to almost 380 million urban residents (UN-Habitat, 2014). Globally, hydrologic regimes leading to urban flooding are varying with climate change (Desai et al., 2015; UNEP, 2016; Willems et al., 2012), and locally, socioeconomic factors associated with urban development (variations in population growth, development, land use and urban density) are uniquely altering each city's individual response to these changing flood levels and frequencies (Desai et al., 2015). In the next few decades, cities will need to anticipate and adapt to this combination of shifting quantities of water and city features (Revi et al. 2014; Doocy et al., 2013). In this study, we aim to develop an understanding of the prevalent global patterns of human-environmental relationships influencing city-level river flooding, and discover how a global set of individual cities fits into these patterns.

Climate change and urbanization are combining to force more frequent flooding and higher flood peaks in cities, though the influence of each factor varies spatially and temporally (Desai et al., 2015). Historically, cities have formed near rivers and population density is still highest, globally, where the closest water feature is a large river. As cities grow, the proximity of population and property to these water courses increases (Kummu et al., 2011). It is estimated that 70% of the world's population will live in cities by 2050 (UN-Habitat, 2010), up from 54% in 2015 (UN-DESA, 2015). With this rapid urbanization, highly populated areas are experiencing an increase in flood vulnerability (Kreimer et al., 2003), as unplanned expansion often leads to migration into urban flood plains (Jongman et al., 2012; Revi et al., 2014). Global urban land cover is increasing at a rate over double that of urban population growth (Angel et al., 2010a) and is projected to increase three-fold by 2030 (Pachauri et al., 2014). More impervious areas and encroachment into the surrounding countryside are forcing faster concentrations of rainfall in urban rivers during storm events, as well as higher flood peaks (Desai et al., 2015; Doocy et al., 2013; Kreimer et al., 2003).

Hydrology in cities is also affected by increased surface temperatures associated with climate change. Already, increases in the frequency and intensity of precipitation (Frich, et al. 2002; Desai et al., 2015; UNEP, 2016), changes in spatial and temporal storm patterns (Wasko & Sharma, 2015) and changing snow melt conditions (Schiermeier, 2011; Barnett et al., 2005; Immerzeel et al., 2010) are leading to variations in the magnitude, frequency and timing of urban river floods, with higher peak flows and shorter response times (Shiermeier, 2011; Cunderlik, 2009). These changing patterns of precipitation and runoff are complex and not uniformly spatially distributed (Meehl et al., 2005; Desai et al., 2015; Wentz et al., 2007; Frich et al., 2002). In the future, cities in particular are predicted to become even more vulnerable to extreme hydrologic events as a result of climate change (Pachauri et al., 2014; Willems et al., 2012; Revi et al., 2014, Sofia et al., 2016). Increases in rainfall intensity at urban hydrology scales of up to 60% are anticipated by 2100 (Willems et al., 2012), and the micro-climates of cities are expected to interact with climate change in a variety of ways, potentially exacerbating flood effects (Revi et al., 2014).

In this paper, a comparison is made amongst a selection of cities based on their current and projected future urban river flood impacts on population and property, resulting from an anticipated combination of climate change and development. It should be noted that fluvial flooding is the only type of flooding that is considered here, and this study does not include an analysis of cities subject to coastal or pluvial flooding. Analysing data with city-specific projections of changes in hydrology, population and development levels (based on future

1 climate scenarios, projected development pathways, and a best assumption of flood protection standards) we
2 produce an analysis and visualisation of the patterns of baseline conditions and anticipated changes in city-level
3 river flooding impacts to the year 2030. We establish the prevalent global spatial and temporal patterns of urban
4 flood impacts, explore these impacts as resulting from both developmental and hydrological drivers, and match
5 the cities to their most similar pattern. The patterns are established through dimension reduction, clustering and
6 visualisation of multivariate data with an adaptation of the self-organizing map (SOM) technique. The SOM is an
7 artificial neural network useful for exploring nonlinearly related variables, and is popular for investigating
8 potentially difficult-to-define environmental responses to human influences (e.g. Shanmuganathan et al., 2006;
9 Vaclavik et al., 2013; Clark et al., 2016b) as well as providing comparisons between geographic areas (Kaski &
10 Kohonen, 1996; Clark et al., 2015; Clark et al., 2016). We begin by presenting analyses of patterns of urban flood
11 conditions (as measured by the amount of population affected and urban damages costs) for a baseline global
12 snapshot (2010), then investigate projected temporal changes (up to 2030), and finally combine this information
13 into a global temporal analysis of the cities. As individual cities are matched to their closest patterns at each
14 stage, we discover clusters of cities with similar urban flooding characteristics and projected trends.

15 A growing body of research is investigating the impact of anthropogenic changes on urban flooding at regional
16 and global scales, however we have found no literature comparing specific cities in terms of changing city-level
17 flood impacts on populations and property. The Intergovernmental Panel on Climate Change's 5th Assessment
18 Report Chapter 8 'Urban Areas' (Revi et al., 2014) discusses the vulnerabilities and resilience of cities to climate
19 change in general, noting that the analysis is based on economic losses and would differ if a human component
20 is included. Jongman et al. (2012) investigated global trends of coastal and river flooding based on changing
21 regional population densities and land use. Increased vulnerability to flooding is attributed to population growth
22 or increases in wealth, though the modelling does not include changing hydrology due to climate change.
23 Jongman et al. (2015) estimated regional trends in human and economic river flooding vulnerabilities by income
24 level, through hazard and exposure calculations. Kunkel et al., (1999) investigated the increasing trend of
25 economic losses and fatalities in the USA due to increasing vulnerability to floods, however the climate change
26 contribution to this increase was not possible to quantify due to a lack of data. Winsemius et al. (2016) produced
27 the first projections of global future flood risk that consider separate impacts of climate change and
28 socioeconomic development, with results discussed by geographic region (river basin) and economic level. The
29 investigation of the connection between coastal flooding and climate change (increasing storms combined with
30 sea level rise) is more common in the literature than the connection between river flooding and climate change
31 (Nicholls et al., 2008; Nature, 2016) due to better data availability. Most existing river flood assessments are at a
32 local or regional scale (as in Muis et al., 2015), limiting the possibility to compare between multiple cities, as
33 studies at a global scale have traditionally been limited by a lack of datasets and methods. Sofia et al (2016)
34 emphasize that analyses of climate change and socio-economic development as both drivers and receptors of
35 flood risk is needed. Muis et al. (2015) call for an investigation between the combination of land use change and
36 hydrologic change on future flood risk. (Jongman et al., 2012) highlight that due to population growth and
37 climate change, global methods incorporating both spatial and temporal dynamics to investigate inland flooding
38 at the city scale are necessary for global development studies and estimating costs associated with climate
39 change. To date, a global examination of changing flood conditions at the city level resulting from urban
40 development and climate change, including a direct comparison between specific cities, has not been made. The
41 analysis we present here corresponds directly to this gap in the literature.

42 General patterns as well as specific relationships can be extracted from the output maps in this paper. In the
43 interest of channelling the 'potential of visual communication to accelerate social learning and motivate
44 implementation of changes' (Sheppard, 2005) the aim of the method used here is to discover and demonstrate

1 potentially interesting global patterns and relationships that would not otherwise be evident in the data, for
2 example: clusters of cities which are currently experiencing high flood impacts that are projected to greatly
3 increase in the future, and to what extent this may be due to climate change (or socioeconomic development)
4 within each city; which cities not currently experiencing notable effects of flooding may expect to in the future;
5 which cities are projected to mitigate potentially adverse flood effects from climate change with reductions in
6 flooding due to socioeconomic factors; which cities are projected to experience an increased flood vulnerability
7 driven by socioeconomic factors alone; and the relationship between the changes in vulnerability of the
8 population and urban damages costs for each city.

9 The comparison of individual cities in this study (rather than river catchments) allows a blending of
10 environmental and social information which reinforces the co-dependence of humans and their natural
11 environment, a relationship which is often easily overlooked by urban dwellers. Explicitly visualising the role that
12 urbanisation may have on the environmental conditions experienced by urban citizens is an essential reminder
13 of this connection. Cities potentially facing similar circumstances and challenges are identified in this study,
14 suggesting possibilities for a sharing of strategies. As climate change, development, and urban administrations
15 transcend river basin boundaries, an investigation of impacts and determination of potential mitigation
16 strategies at the city level as well as the basin level expands the potential for decision makers to be presented
17 with all the available, relevant data for consideration.

18 2 DATA AND METHOD

19 DATA

20 The data set used in this study combines city-level estimates of annual expected urban river flood impacts on
21 population and urban damages costs (2010), projections of future changes in flood impacts attributed to climate
22 change and/or development (up to 2030), and socioeconomic data for a globally distributed set of cities.

23 The selection of cities used here is based on a list provided by the Lincoln Institute of Land Policy's Atlas of Urban
24 Expansion (Angel et al., 2010, website 1), spanning all continents except Antarctica, encompassing four economic
25 levels and four population levels. City population data (2010) and future population estimates (2030) are from
26 the UN Department of Economic and Social Affairs (UN-DESA, 2015), and GDP per country are from the World
27 Bank's World Development Indicators database (website 2).

28 Annual river flood impact estimates are obtained from the global dataset of fluvial flood risk published in the
29 World Resources Institute's Aqueduct Global Flood Analyzer Tool (herein referred to as Aqueduct) (Winsemius
30 et al., 2013; Ward et al., 2013; website 3). Released in 2015, this data set comprises the first unified global set of
31 fluvial flood risk data at the city level. As this data is solely related to the influence of fluvial flooding on
32 metropolitan areas, it does not include coastal or pluvial flood risks. In this data set, Aqueduct provides separate
33 estimates of annual impacts on the number of affected population (people exposed to flood waters) and urban
34 property damages costs (in US dollars), which will be referred to in this paper as 'population' and 'damages'
35 impacts.

36 Global hydrologic and hydraulic models, inundation modelling, and spatial data sets of population, land use and
37 infrastructure are used within Aqueduct to quantify flood risk in each city. Aqueduct identifies future anticipated
38 changes in urban flood vulnerabilities as driven by climate change (altered hydrology), socioeconomic
39 development (population, land use and economic changes), or in most cases a combination of both. Either of
40 these drivers may increase or decrease the frequency and intensity of flooding, and the resulting flood impacts,
41 for a given city. Three separate scenarios of climate change and socioeconomic development (optimistic,

1 business-as-usual, and pessimistic) are given in Aqueduct, and in this study we use data from the business-as-
 2 usual case for our future flood impact scenario. Future hydrologic and hydraulic estimates in Aqueduct are based
 3 on global circulation model data from the ISIMIP project (website 4) and changes in population and economic
 4 development are based on Shared Socioeconomic Pathways data with a downscaling procedure that
 5 differentiates between urban and rural growth (website 5; Samir & Lutz, 2014). Recent papers published with
 6 this data include Winsemius et al. (2016), Jongman et al. (2015) and Muis et al. (2015).

7 Expected flood impacts are provided by Aqueduct for nine possible levels of city-wide flood protection, from
 8 protection against the 2-year average return interval (ARI) flood to the 1000-year ARI flood. This protection level
 9 indicates how well protected the area is against flood damage, based on the standard or capacity of flood
 10 protection measures such as dikes, levees or dams. In this study, we assign an assumed flood protection level to
 11 each city based on the country's World Bank income level (as in the World Resource Institute's Aqueduct Global
 12 Flood Risk Country Rankings, website 6) due to a lack of information on each city's actual protection level. This
 13 method follows recommendations based on the rational that higher standards of protection against flooding
 14 may be expected in higher income countries (Jongman et al., 2012; Nicholls et al., 2008), and findings by Doocy
 15 et al. (2013) that flood impacts are significantly associated with classification of income level by the World Bank.
 16 We assume each city's flood protection level remains the same during the timeline of this study.

17 To allow for a comparison between cities of greatly differing sizes and hydrologic conditions, the wide-ranging
 18 data values were log-transformed. The data set was then standardized by transforming these values linearly into
 19 the range 0-1 (with the lowest value becoming 0 and the highest value becoming 1) for each variable (population
 20 affected, urban damages, etc). The data is log transformed, following recommendation by Agarwal & Skupin
 21 (2008) that highly skewed variable distributions may benefit from log transformation before use in the SOM.
 22 Cities with no flood impacts in both 2010 and 2030 were removed (22 cities), though cities with no flood impacts
 23 in 2010 but with flood impacts in 2030 have been kept in the study. The final list of cities is presented in Table 1.

24 **TABLE 1: CITY LIST** - alphabetically by region.

Eastern Asia & the Pacific		South Asia		Zugdidi	Georgia
Anqing	China	Dhaka	Bangladesh	North Africa	
Ansan	Rep. of Korea	Hyderabad	India	Alexandria	Egypt
Beijing	China	Jalna	India	Algiers	Algeria
Changzhi	China	Kanpur	India	Aswan	Egypt
Chinju	Rep. of Korea	Kolkata	India	Cairo	Egypt
Fukuoka	Japan	Mumbai	India	Casablanca	Morocco
Guangzhou	China	Puna	India	Marrakech	Morocco
Leshan	China	Rajshahi	Bangladesh	Port Sudan	Sudan
Pusan	Rep. of Korea	Vijayawada	India	Tebessa	Algeria
Seoul	Rep. of Korea	Western & Central Asia		Sub-Saharan Africa	
Shanghai	China	Ahvaz	Iran	Accra	Ghana
Sydney	Australia	Astrakhan	Russian Fed.	Bamako	Mali
Tokyo	Japan	Baku	Azerbaijan	Harare	Zimbabwe
Ulan Bator	Mongolia	Gorgan	Iran	Ibadan	Nigeria
Yiyang	China	Istanbul	Turkey	Johannesburg	South Africa
Yulin	China	Kuwait City	Kuwait	Kampala	Uganda
Zhengzhou	China	Malatya	Turkey	Kigali	Rwanda
Southeast Asia		Moscow	Russian Fed.	Ouagadougou	Burkina Faso
Bandung	Indonesia	Oktyabrsky	Russian Fed.	Latin America & the Caribbean	
Bangkok	Thailand	Sanaa	Yemen	Buenos Aires	Argentina
Ho Chi Minh City	Vietnam	Shimkent	Kazakhstan	Caracas	Venezuela
Kuala Lumpur	Malaysia	Teheran	Iran		
Manila	Philippines	Tel Aviv	Israel		
Palembang	Indonesia	Yerevan	Armenia		
Songkhla	Thailand				

Guadalajara	Mexico	Cincinnati	United States	Castellon	Spain
Ilheus	Brazil	Houston	United States	Le Mans	France
Jequeie	Brazil	Los Angeles	United States	Leipzig	Germany
Mexico City	Mexico	Minneapolis	United States	London	UK
Montevideo	Uruguay	Modesto	United States	Madrid	Spain
Ribeirao Preto	Brazil	Philadelphia	United States	Paris	France
Santiago	Chile	Pittsburgh	United States	Sheffield	UK
Sao Paulo	Brazil	Springfield	United States	Thessaloniki	Greece
Tijuana	Mexico	St. Catharine's	Canada	Warsaw	Poland
Valledupar	Colombia	Tacoma	United States	Wien	Austria

North America
Chicago United States

Europe
Budapest Hungary

1

2 METHOD

3 We use an extension to the self-organizing map method to determine patterns and similarities in the impacts,
 4 changes and drivers of urban flooding amongst the cities. The self-organizing map (SOM, Kohonen, 2001) is an
 5 unsupervised learning algorithm from the family of artificial neural networks that discovers patterns in
 6 multivariate data sets with nonlinear inter-variable relationships.

7 The SOM reduces the dimensionality of the data set by creating a (in this case) two-dimensional map grid which,
 8 through an iterative process, is essentially bent and stretched over the data set until it best characterizes the
 9 shape of the data cloud. The numerous data items become represented by a (usually) much smaller number of
 10 map nodes, known as prototypes. The map nodes, or prototypes, move iteratively into position amongst the
 11 data whilst maintaining their grid formation, establishing a higher density of prototypes in areas of higher data
 12 density. Once in position, the prototypes represent the most prevalent patterns in the data. Each data item is
 13 then matched to its closest prototype, creating clusters of similar data items.

14 The SOM algorithm consists of a two-step iterative process of comparing the map and the data, and then
 15 updating the map to better represent the data. The method begins with a calculation of distances in data space
 16 (in this case we use Euclidean distance) between each data item, x_i (where $i = 1:N$), and each map node, m_j
 17 (where $j = 1:M$). Data and map nodes vectors are all of the same dimension, d . The goal of the comparison
 18 stage is to find the nearest map node to each data item (commonly referred to as the best matching unit, BMU),
 19 which is then given the index c , using the following calculation:

20
$$\|x_i - m_c\| = \min_j \{\|x_i - m_j\|\} .$$

21 This partitions the data into subsets of items sharing the same nearest node, m_c . Next, the locations of the
 22 map nodes are adjusted to become closer to their nearby data items. Application of a smoothing
 23 ‘neighbourhood’ kernel during this stage produces a smoother map by updating neighbouring nodes to a
 24 similar extent based on the nearby data. That is, the location of each map unit, m_j , becomes updated based
 25 on a weighted average of the data items matching itself as well as its neighbouring nodes, where the
 26 weighting is given by the neighbourhood kernel. The size of the kernel decreases with each iteration to include
 27 fewer nodes. We use a Gaussian shaped neighbourhood kernel, where h_{ij} (the neighbourhood kernel
 28 element indicating the influence of each data item, x_i , on the updating of node m_j) is defined at iteration t as:

29
$$h_{ij}(t) = \exp\left(\frac{-(m_c - m_j)^2}{2\sigma^2(t)}\right)$$

30 where σ is the kernel radius. At each iteration (t), the updated node locations are found as in (Kohonen, 2013):

$$m_j(t + 1) = \frac{\sum_{i=1}^N h_{ij}(t) x_i}{\sum_{i=1}^N h_{ij}(t)}.$$

After map training is complete, the map node vectors each represent a unique combination of variables in the data, according to the final location of the map nodes in data space. Each of these unique combinations of variables represents a characteristic pattern in the data. The data items are once again matched to their closest map node, forming clusters of data that best match each pattern.

In this study, the ‘patterns’ are the key characteristics represented by each map node vector (such as specific baseline and/or projected flood conditions, and the drivers of change). The ‘cluster’ members are the cities that match the pattern represented by their nearest map node better than they match the patterns of any other nodes.

As the SOM is an unsupervised learning algorithm, there is no subjectivity in the resulting cluster memberships. The iterative training process discovers the principal curves of the data set (the nonlinear directions of maximum variance) and aligns the map coordinate system with these, so that the two axes of the map generally follow the first two principal curves of the data. When the map is presented in its two-dimensional form, with data items located at their nearest map node, similar data ends up in close proximity on the map and dissimilar data is far apart. Through the SOM creation process the prevalent data patterns are identified by the nodes, data items become grouped into clusters around these patterns, and the clusters are ordered by similarity on the map. For a more detailed summary of the SOM method, refer to e.g. Clark et al. (2015).

In this study, the data set is split into two subsets (‘baseline’ data and ‘projected future changes’) for each city, allowing a progressive investigation of spatial and temporal patterns of urban flooding. A series of three separate SOMs (also referred to as maps) are created with prevalent global patterns and city similarities established separately on each map through colouring and labels, as follows:

- SOM1 explores the spatial properties of the baseline data set, enabling a comparison of the state of urban river flood impacts in each city at a snapshot in time (2010).
- SOM2 explores patterns of projected temporal changes in impacts of urban flooding on population and property (to 2030), incorporating the drivers of climate change and urban development, and
- SOM3 portrays the temporal relationships between the cities in a type of longitudinal exploratory data analysis, clustering cities that are similar in the baseline situation and are also projected to trend similarly in response to each driver in the future.

SOM1, the baseline map, depicts prevalent global spatial patterns and identifies urban flooding conditions in each city based on two variables: 1) the total population affected annually by river flooding, and 2) annual urban property damages costs incurred by river flooding. The map is created based on these two variables, though by projecting new variables onto the trained map it is also used to show: 3) the percentage of each city’s population affected, and 4) the percentage of the country’s GDP affected. Usually used with higher-dimensional input data, the SOM method is useful here for creating a map with two variables as the nonlinear projection establishes the relationships between cities in alignment with the directions of maximum variance (ie. the directions of most importance) in the data. It also allows for the results to be used as input into SOM3 later.

SOM2, the future projected changes map, describes the anticipated alterations in urban river flooding in each city by 2030. This map is based on four variables of projected changes and their associated drivers: 1) the projected change in population affected annually, 2) the projected change in annual urban damages costs, 3) the proportion of change in population affected that is anticipated to be attributable to climate change, and 4) the

1 proportion of change in urban damages costs that is anticipated to be attributable to climate change. The
 2 remainder of the increase or decrease in impacts is attributed to socioeconomic causes (such as population
 3 change, urban density change, increased city footprint, and changes in urban land cover).

4 SOM3, the temporal map, uses the location of each city along the axes of the two-dimensional baseline and
 5 future projected changes maps (which essentially delineate the first two principle curves in each higher
 6 dimensional data subset) as input data. In creating SOM1 and SOM2, the baseline and future data subsets have
 7 already been reduced to their two most prominent dimensions respectively (which have become the axes of
 8 these maps), and each of these four dimensions is considered equally when placing the cities on the temporal
 9 map. This method is based on the method used in Clark et al. (2015) to investigate individual data items
 10 transitioning through a self-organizing-time-map, and has been modified for the comparison of patterns on two-
 11 dimensional maps of differing sizes and shapes that have been created separately based on different variables.

12 Distinct patterns that have emerged through the process of training the three maps are represented by the
 13 nodes of SOM3. These patterns are the most relevant combinations of dynamic city flood impacts,
 14 socioeconomic, and climate change characteristics in the overall data set. SOM3 is clustered, coloured and
 15 labelled to indicate the relationships between the cities in terms of similar or differing baseline situations *and*
 16 projected changes. Cities with relatively close locations on both the baseline and future projected changes maps
 17 are considered to have parallel temporal paths, and will be found close together on the temporal map. Those
 18 with converging trends (dissimilar baseline conditions, but similar future projected changes) and diverging
 19 trends (close baseline conditions, but dissimilar future projected changes) are also identifiable on this map.

20 In the creation of each map, grid size and shape have been determined using quantization, topographic and
 21 dimension range representation error measures (QE, TE, and DRR) with comparisons between the data set and
 22 the map.

23 The QE (Kohonen, 2001) measures how well the map nodes represent the data items using the sum of squared
 24 Euclidean distances between each data item, x_i , and the node closest to it, m_c , averaged over all data points:

$$25 \quad QE = \frac{1}{N} \sum_i \|m_c - x_i\|^2 = \frac{1}{N} \sum_i \sqrt{(m_c^2 + x_i^2 - 2m_c x_i)}.$$

26 The TE (Kiviluoto, 1996) indicates how well the topography of the data set is preserved on the map, giving higher
 27 error values for maps that are unnecessarily bent or twisted. The BMU and second BMU for each data point are
 28 checked to determine if they are adjacent ($u_{x_i} = 1$ if the first and second BMUs of x_i are neighbours, 0
 29 otherwise), and TE is calculated as:

$$30 \quad TE = \frac{1}{N} \sum_{i=1}^N u_{x_i}$$

31 The DRR (Clark et al., 2015) measures how well the map represents each variable of the data set to ensure even
 32 coverage of the dimensions. The maximum intra-cluster spread of data items in each dimension, d , that become
 33 represented by a single map node, x_i (as a proportion of the overall data range in that dimension) is determined.
 34 The DRR is calculated as follows, where $x_i(d)$ are data values in dimension d , and $x_{ij}(d)$ are the data values in
 35 dimension d that are assigned to map unit j :

$$36 \quad DRR(d) = \max_j \frac{\max_{ij} (x_{ij}(d)) - \min_{ij} (x_{ij}(d))}{\max_i (x_i(d)) - \min_i (x_i(d))}$$

1 For the baseline map, a 10*7 grid is found to be the optimum shape to represent the data based on the error
2 measures. An 8*8 map is fitted to the future projected changes data set. After finding these optimum side ratios,
3 the maps are increased in size preserving their side ratios (to 20*14 and 18*18) to allow the data items to spread
4 out until most cities are placed individually, allowing the relationships between all cities to become evident (as
5 in Skupin & Hagelman, 2005). The temporal map is sized at 25*17 nodes. Whilst the input data for the baseline
6 and future projected changes maps were standardized into the range 0-1 before training, the input data for the
7 temporal map is not standardised in order to preserve the ratios between the lengths of the first two principal
8 curves in each of the first two data subsets.

9 Prevalent cluster characteristics are determined using a ‘second level’ clustering of the nodes of the SOM (as in
10 Vesanto & Alhoniemi, 2000; Skupin & Hagelman, 2005), performed using Ward’s clustering method (Ward, 1963)
11 with the number of clusters determined using the Davies-Bouldin index (Davies & Bouldin, 1979). The Davies-
12 Bouldin index reports the ratio of within cluster scatter (S_j for cluster j) to inter-cluster distances, looking at
13 each cluster and its most similar one, (M_{jk}), with a lower ratio (S_j/M) indicating a better estimate of the number
14 of clusters of interest present in the data. Ward’s minimum variance method is a hierarchical clustering algorithm
15 based on minimizing the total within-cluster variance. With this second-level clustering, each data item of the
16 original data set becomes a member of the same final cluster as its closest node (Vesanto & Alhoniemi, 2000).

17 The final clustering is visually verified with a SOM ‘U-matrix’ (Ultsch, 2003). The U-matrix visualises distances in
18 data space between immediately neighbouring nodes, indicating these distances by colour on a grid of the same
19 size as the SOM. By computing how close adjacent map nodes are in data space, the U-matrix is able to provide
20 an indication of cluster boundaries based on large dissimilarities between neighbouring nodes. A greater change
21 in relative distance between the locations of the nodes in data space than in map space is displayed in a lighter
22 colour on the grid, and lesser distances in darker shades. The darker regions of the grid then indicate the cluster
23 centres, separated by lighter coloured boundary areas.

24 By reducing the information from this multivariate data set into the two most prominent dimensions and finding
25 relationships between the data items at each of these three stages, spatial and temporal information about
26 global patterns of urban flooding is abstracted, and similarities and differences between the cities are clearly
27 portrayed. This method extracts two levels of information:

- 28 (1) the most characteristic socio-environmental patterns in the data are found, and
- 29 (2) cities are compared to each other with respect to their relative flooding conditions.

30 The simulations are run in Matlab with use of the SOM Toolbox (website 7) with variables and map sizes as
31 described above.

32 3 RESULTS

33 Three SOMs are presented sequentially to reveal three unique sets of patterns in the data, where the term
34 ‘patterns’ refers to combinations of variables that characterise a specific set of conditions. The cities are
35 clustered into groups with conditions matching these patterns, based only on the given data. The maps each
36 have different sizes, shapes and colours as they represent different subsets of input data.

37 SOM1: BASELINE URBAN FLOOD IMPACTS

38 Patterns of urban flood conditions in 2010 are shown on the baseline map, SOM1, in Figure 1. The placement of
39 city labels indicates the relationship of each city to each other in terms of river flood impacts on population and

1 urban damages costs. The map is created by organizing the cities with respect to each other based on both of
2 these factors. Cities close together are more similar in the amount of population affected and urban damages
3 costs, and cities located far apart are less similar.

4 The relative placement of the cities on the map is the main map characteristic providing insight into the features
5 of the data, indicating differences in a *combination* of the variables which can be discerned from the colouring
6 of Figure 1(a). Each map node has a four-component vector (representing the value of each of the four variables
7 at the location of the node in data space). The four images in Figure 1(a) show SOM1's city labels over grids
8 coloured separately by the values of each of the four variables (white is low, purple is high). For each city, the
9 relative value of each of the variables can be seen. For example, Cincinnati (top right) incurs high material
10 damages costs, and medium population affected, whereas Ulan Bator (mid left) has similar population affected
11 to Cincinnati, but much lower material damages costs.

12 The nonlinearity of the relationships between the variables is evident, as is the smooth transition of the values
13 of each variable along the map. General information about the prevalent baseline global patterns and the relative
14 flood conditions in the specific cities can be gained from inspection of these map labels and coloured grids.

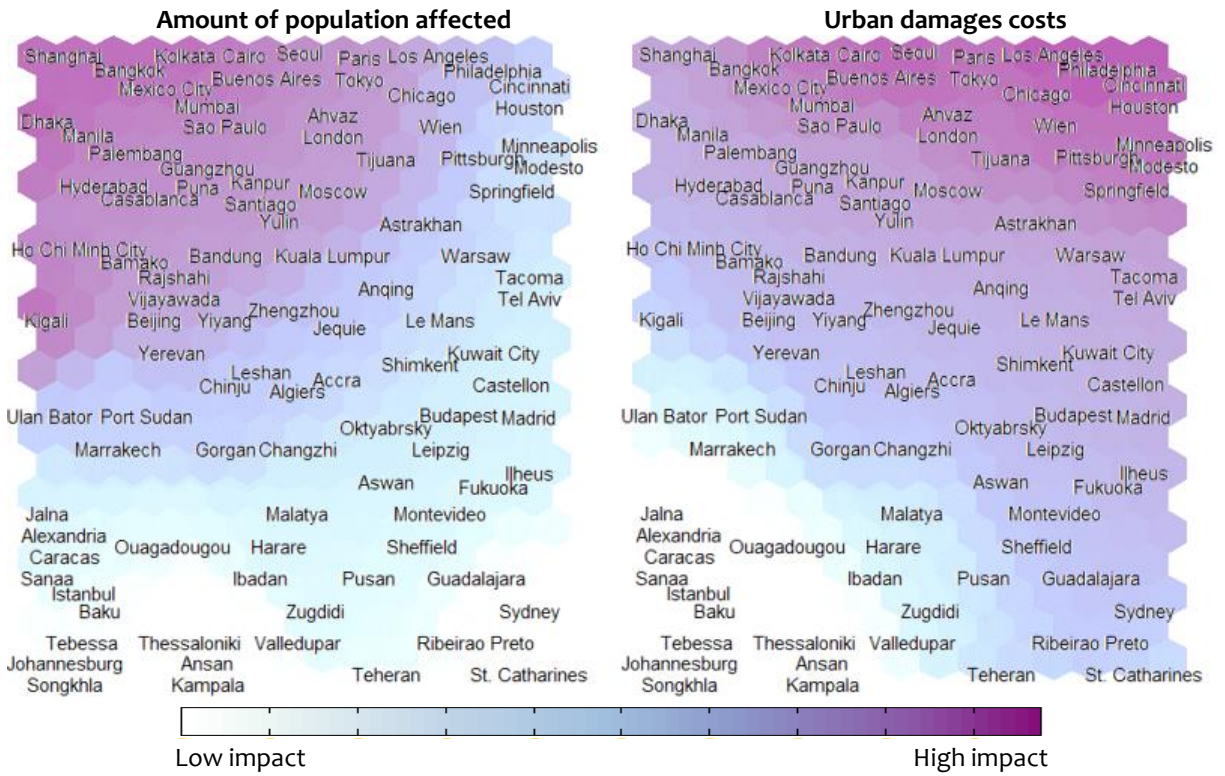
15 Each area of the grid represents a general pattern, or combination of variables in the data, some of which are
16 indicated by annotations on Figure 1(b). In general, higher amounts of population affected and urban damages
17 costs resulting from river flooding are represented by areas towards the top of the map, and these variables
18 decrease in value down the map. Values of affected population are lowest just in from the lower left corner and
19 undulate along the bottom of the map, sweeping upwards to a maximum at the upper left corner. Urban damage
20 values are lowest in the lower left corner and increase in concentric arcs up to the upper right corner. Generally,
21 the left of the map contains patterns involving higher impacts on populations than on property, and the right of
22 the map higher impacts on property than on populations.

23 From Figure 1(b), relationships can be discerned between regions, as well as between cities in the same region.
24 For instance, cities in North Africa, Sub-Saharan Africa and West & Central Asia are predominantly located in the
25 lower portion of the map, corresponding to a prevalent pattern of low flood impacts on both population and
26 property. Cities in Southeast and South Asia generally correspond to the patterns of high impacts on population
27 and property found in the upper left of the map. Cities in Europe stretch from the top to the bottom of the map,
28 ranging from high overall flood effects (Paris) to no flood effects at all (Thessaloniki). North American cities are
29 matched to patterns that represent more significant impacts on property than on population (down the right
30 side of the map), and are split between those with high property damages (Philadelphia, LA, etc. – in the top
31 right) and those with low damages (St. Catherine's – in the bottom right).

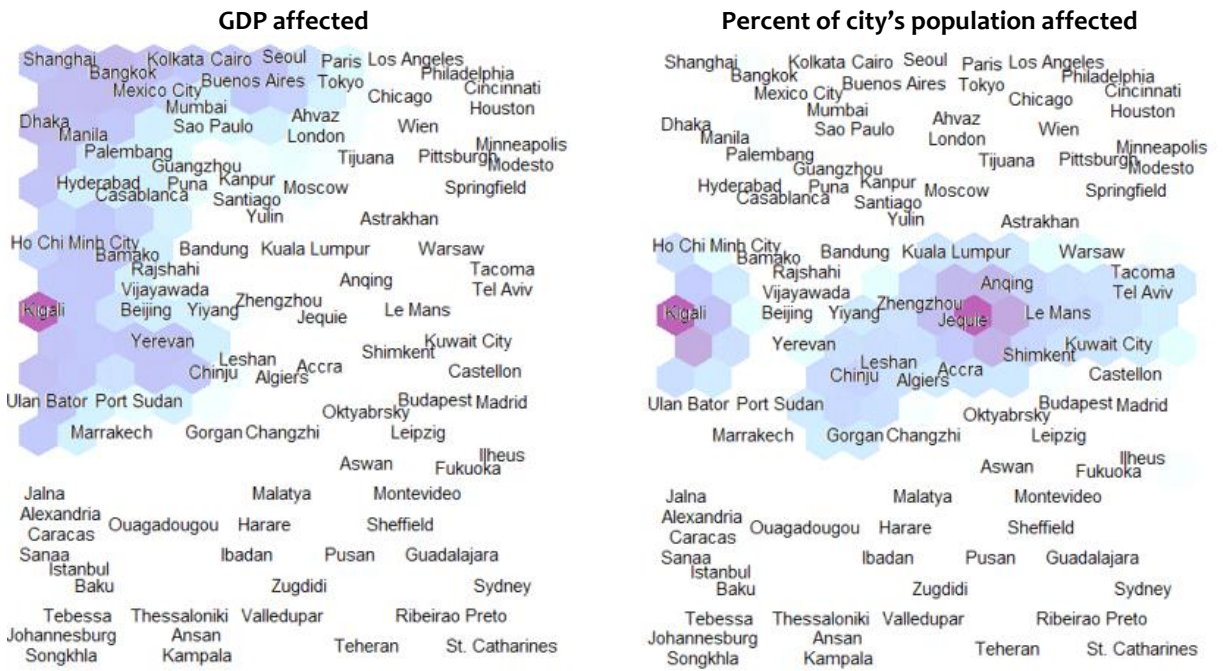
32 Impacts on GDP and the proportion of the cities' populations affected are shown in the two lower maps of Figure
33 1(a), though these variables were not used to position the cities on the map. Cities in which river-related urban
34 flooding is estimated to highly affect the country's GDP are coloured on the lower left map. Kigali, in particular,
35 which incurs medium-high flood impacts, sees a large impact on Rwanda's GDP, perhaps because Kigali is the
36 main city in this relatively small country (Kreimer et al., 2003). GDP is most affected by flooding in: Kigali,
37 Bangkok, Yerevan, Dhaka, Bamako and Cairo. Cities in which the flood-affected population forms a significant
38 proportion of the city's population are coloured on the lower right map, predominantly in a horizontal strip
39 across the centre. The highest proportions are in: Jeju (15%), Kigali (7%), Chinju (6%), Le Mans (5%) and Tacoma
40 (3%).

41

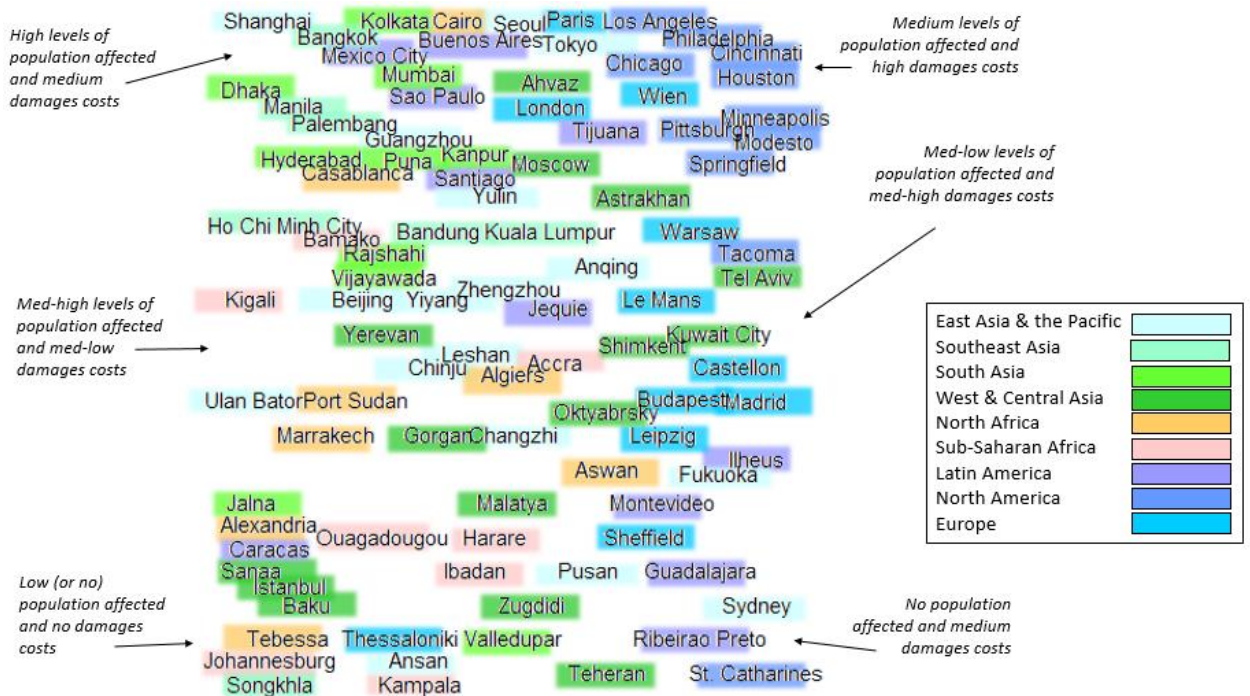
1 a)



2



b)



1

2

3

4

5

6

7

FIGURE 1: SOM1 - BASELINE (2010) URBAN FLOOD CONDITIONS. Cities are placed relative to each other based on annual river flooding impacts on population and urban damages costs. a) The same map is repeated for each of four variables, with colouring indicating low (white) and high (purple) values. b) The city labels are coloured by region (see Table 1), and characteristic patterns of general areas of the map are annotated. The reader may refer to the online version to zoom in on text if required.

8

SOM2: PROJECTED CHANGES IN URBAN FLOOD IMPACTS (TO 2030)

9

10

11

SOM2 identifies the projected patterns of evolving river flood conditions in the cities (between 2010 and 2030), based on city-specific projections of increasing or decreasing flood impacts on population and damages costs, and whether these changes are anticipated to be driven more by climate change or development (Figure 2).

12

13

14

15

16

17

18

In Figure 2(a), regions of the map representing projected increases in flood impacts on either populations or damages costs are coloured blue and reductions in flood impacts are coloured brown (in the top row), with white indicating no projected change. Projected changes primarily driven by socioeconomic development are coloured purple (in the lower row), and green indicates that the primary driver is climate change. White represents a mid-point in which both climate change and development are predicted impact future flood conditions relatively equally. Areas of the map representing patterns of increased flood impacts predominantly due to climate change or development can be located on Figure 2(b).

19

20

21

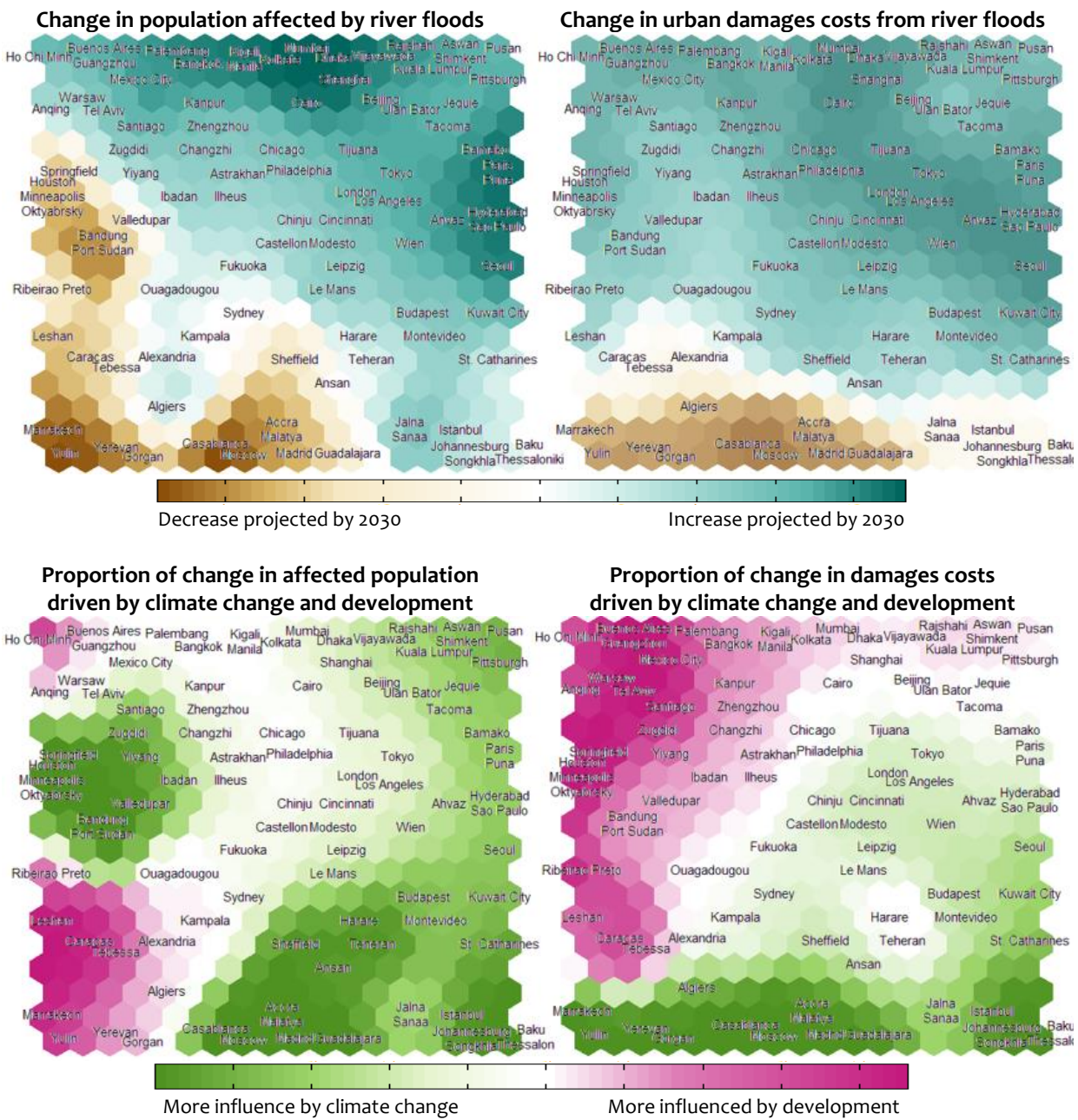
22

23

Investigating SOM2, we see that climate change is projected to be predominantly responsible for increases in population vulnerability in all cities besides those in the top left corner (around Ho Chi Minh City). Climate change is anticipated to decrease flood damages costs in cities located at the bottom of the map (around Madrid), and decrease impacts on populations in cities in the mid-left (around Minneapolis) and mid-lower (again around Madrid) portions of the map. Socioeconomic development is projected to be the main driver increasing flood

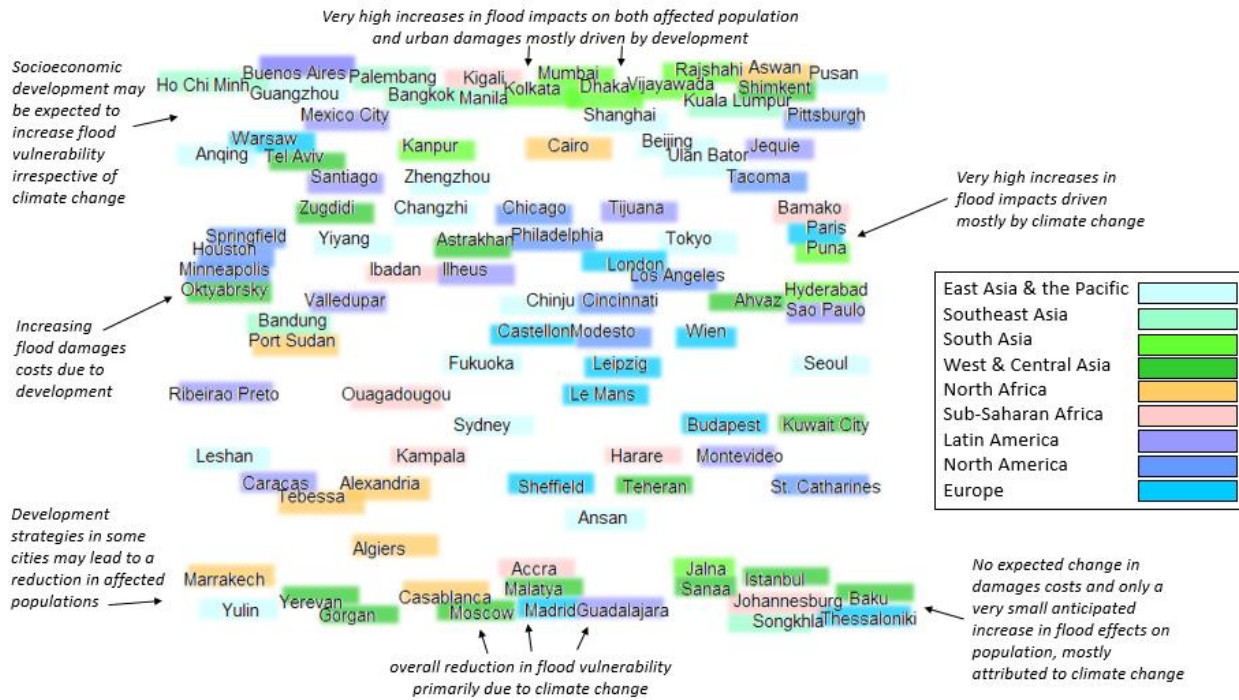
1 damages costs in cities on the upper-left triangle of the map (roughly from Mumbai down to Tebessa). Only in
 2 Ho Chi Minh City is development anticipated to be almost completely responsible for all increases in river flood
 3 impacts, all other cities in this study are at least partially affected by climate change. Development is not
 4 projected to play any part in a decrease in flood damages costs in any cities in this study (Caracas and Tebessa
 5 have no change in damages costs on the upper map, though it is attributed to development on the lower map).

6 a)



7

b)



1 **FIGURE 2: SOM2 - PROJECTED CHANGES IN RIVER FLOOD IMPACTS WITH ASSOCIATED DRIVERS.**

2 River flooding in individual cities will be affected separately by climate change and development
 3 between 2010 and 2030. Cities that are anticipated to experience similar pressures and responses in
 4 terms of river flooding impacts are located nearby on the map. a) City labels are placed over coloured
 5 copies of the map showing the relative values of each variable. b) City labels are coloured by region,
 6 and characteristic patterns of general areas of the map are annotated. The reader may refer to the
 7 online version to zoom in on text if required.

8 Geographic regions are shown on Figure 2(b) with coloured text backgrounds. Cities in Southeast Asia are almost
 9 all found at the top of the map indicating high projected increases in overall flood impacts. South Asian cities are
 10 mostly located in the two areas of the map with patterns of very high increases in flood impacts, split between
 11 those most affected by development (around Mumbai, top middle) and those most affected by climate change
 12 (around Puna, mid right). Many North African cities are located in the lower left, indicating anticipated reductions
 13 in flooding due to socioeconomic development. North American cities are spread across the middle of the map
 14 indicating a wide range of projected changes.

15 Climate change and development may lead to opposing changes in a city's flood impacts on population and
 16 property. A number of cities are predicted to have affected populations decreasing due to climate change, whilst
 17 damages costs increase due to socioeconomic factors (around Springfield and Port Sudan, in the mid-left). A
 18 decrease in flood effects on urban damages due to climate change, but an increase in affected population largely
 19 due to development is, out of the cities in this study, only projected for Algiers (in the lower left portion of the
 20 map).

21 In some cities, both drivers may generate changes in the same direction. For instance, in Marrakech, Yulin,
 22 Yerevan and Gorgan, climate change is projected to be responsible for a decrease in damages costs whilst
 23 socioeconomic development is anticipated to play a major role in the decrease in population affected, suggesting

1 that the reduction of population vulnerability due to development is complementing the direction of change
2 instigated by climate change. In certain cities near the upper left of the map (Santiago, Zugdidi and Yiyang), an
3 overall increase in flood impacts is expected, with increases in affected population almost completely attributed
4 to climate change and increases in damages costs almost completely attributed to development.

5 **SOM₃: TEMPORAL PATTERNS**

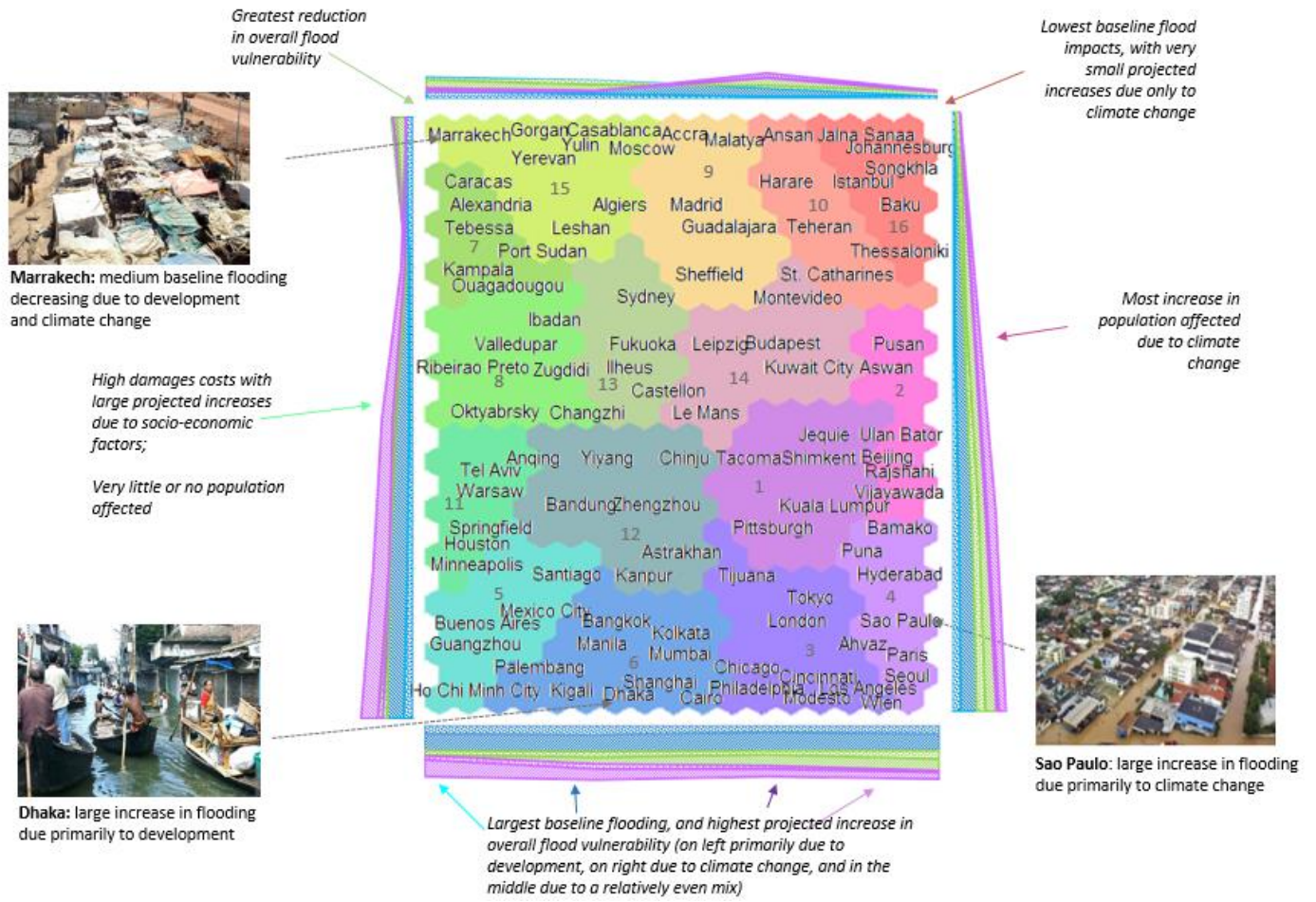
6 Relationships between the baseline characteristics and projected future changes of urban flooding in the
7 individual cities are shown in Figures 1 and 2 respectively, however potentially similar temporal patterns between
8 the cities are not evident from these maps. To link the information abstracted from the first two maps, we create
9 a temporal map, SOM₃, shown in Figure 3. SOM₃ identifies which cities experience similar baseline flooding, are
10 expected to incur comparable future hydrologic pressures from climate change and/or development, and are
11 projected to respond in similar ways (or which cities may diverge in the future from similar baseline conditions).

12 Following the creation of SOM₃ and the positioning of cities with respect to each other, we perform a second
13 level clustering to colour the nodes, giving a visual separation to groups of more similar data. Clusters are
14 numbered from 1 to 16 for reference. As the cities are placed on the temporal SOM based on their locations on
15 the baseline and future projected changes SOMs (in which the values of the variables vary smoothly though not
16 monotonically along the axes), again the characteristics of the cities will flow smoothly along the map though
17 multiple peaks and troughs of each variable are possible. The gradients of the cluster characteristics are indicated
18 along the axes in Figure 3(a), which are nonlinear in data space.

19 Broad overviews of the patterns represented by certain regions of the map are identified on Figure 3 with arrows.
20 The largest increases in flood effects are generally represented by nodes in the lower half of the map, whilst the
21 largest decreases in flood effects are represented by nodes in the top left. Climate change is predicted to be the
22 main driver of changes in population vulnerability along the top and down the left and right sides of the map,
23 and in urban damages on the top and right of the map; therefore, climate change is the leading driver of changes
24 in flood impacts on both population and damages costs at the top of the map. Development is the main driver
25 of changes in flood impacts on populations in the lower and upper left side of the map, and on urban damages
26 in the lower left area of the map; therefore, development is the leading driver of changes in flood impacts on
27 both population and damages costs in cities on the lower left side of the map.

28 On Figure 3(b) the city labels are coloured by geographic region. We see the cities of each geographical region
29 are more spread out on SOM₃ than on SOM₁ where each region was generally contained in one or two broad
30 areas of the map. For example, on SOM₃ Cairo and Aswan are noticeably separated from other North African
31 cities which are located close together. Although the cities of this region have differing baseline flood levels (as
32 shown on SOM₁), most are projected to incur some reduction in future flood impacts (as shown on SOM₂), with
33 the exception of Cairo and Aswan. These cities both have forecasts of increased flood impacts - for Aswan
34 increased impacts on the population due to climate change and impacts on property due to development, and
35 for Cairo future impacts are projected to increase due to a relatively even mixture of both drivers. For another
36 example, cities in the USA (all of which have similar starting conditions) are in two well-separated clusters on
37 SOM₃ - those around Houston and those around Los Angeles. The cities clustered around Houston are
38 characterised by low impacts on population but high damages costs projected to elevate due to development,
39 implying the possibility for local redemption due to better planning or mitigation strategies. The cities clustered
40 around Los Angeles, however, are characterised by high overall impacts projected to get higher predominantly
41 due to climate change. Further, in Sub-Saharan Africa we see Kigali and Bamako (which have similar medium-
42 high baseline flooding conditions) are both expected to see increased impacts, but the cities are separated by
43 SOM₃ as these flood increases are attributed to development in Kigali and climate change in Bamako.

1 a)



2

3

4

1 b)
2



3
4
5
6
7
8
9
10
11
12

FIGURE 3: SOM₃ - TEMPORAL PATTERNS – Cities are clustered close together that share similar baseline (2010) flood vulnerabilities as well as similar anticipated changes driven by climate change and development on population and urban damages costs by 2030. a) Locations of the cities are based on their individual relationships to the principal curves in the baseline and future projected changes data subsets - therefore, the axes represent the most important nonlinear gradients of flood vulnerabilities in the data set. Coloured bars along the axes indicate the average levels of each variable around the edges of the map. Cities are grouped into coloured clusters based on similarities. b) City labels are coloured by region, and characteristic patterns of general areas of the map are annotated. **The reader may refer to the online version to zoom in on text if required.**

13 To further analyse the characteristics of each cluster and the patterns found on SOM₃, the properties of each
14 city in the 16 clusters are shown in a radial plot in Figure 4. Baseline values of population affected (blue, units =
15 number of people) and damages (orange, units = \$US) are shown on a symmetrical logarithmic scale ranging
16 from -8 (ie. signifying a value of -100,000,000) to 11 (100,000,000,000) with the region between -1 and 1 on the
17 plot set as linear to avoid logarithmic discontinuities in the vicinity of zero. Zero is indicated by a dashed
18 circumference, and each progressive ring is an exponentially higher (or lower) value. Changes in population
19 affected and damages costs are shown on the same scale, in grey and yellow respectively. Values inside the
20 dashed (zero) circle represent decreases in flood impacts, and values outside represent increases, with the size
21 of the increase or decrease indicated by the distance from the dashed circle. The influence of climate change is
22 shown (light green for population and dark green for damages) on a linear scale from the same zero
23 circumference, in units of ‘percentage of projected change attributable to climate change’ (each progressive
24 ring is 10%). Green lines closer to the outer ring than the centre therefore indicate that the flood impacts on the
25 city are anticipated to be more influenced by climate change than by development. If the green lines are both in
26 the middle of the segment, this indicates a relatively equal influence of both drivers on both population and

1 property. Diverging green lines indicate that either population or damages costs are more influenced by climate
2 change, and the other by development.

3 From Figure 4, we can see the differences between neighbouring clusters, such as 10 and 16 located in the top
4 right of the map. Both clusters are characterized by low baseline impacts of flooding on the population, with
5 small increases in population impacts projected primarily due to climate change. However, cities in cluster 16
6 incur no flood damages costs at all in the baseline or future cases, yet in cluster 10 damages costs are projected
7 to increase due to climate change and development. Therefore, development has little or no impact on cities in
8 cluster 16 but does play a role in the increase in damages in cluster 10. In the top left of SOM3, we can now also
9 discern the difference between clusters 9 and 15. In both clusters, development is projected to have no impact
10 on the reduction of flood damages costs in most cities. Development does however play a strong role in the
11 reduction of flood impacts on populations in cluster 15 (except for Moscow and Casablanca) but none on
12 populations in cluster 9.

13 The relationship between the two drivers, climate change and development, can discerned from Figures 3 and
14 4. Climate change is projected to impact populations more than urban damages costs in clusters stretched across
15 the centre of the map (clusters 8, 11, 5, 6, 12, 14, 1, 10, 1, 2, and 4 - in cities in these clusters, the proportion of
16 change in the population affected attributed to climate change is higher than the proportion of change in
17 damages costs attributed to climate change). In cluster 15, the population is projected to be more influenced by
18 development than damages costs will be (a higher proportion of the change in damages costs is attributed to
19 climate change than for population). In the remaining clusters, climate change (and development) are projected
20 to affect the population and damages costs relatively similarly (clusters 7, 13, 9, 16 and 3). Some examples of
21 diverging impacts on population and damages costs stand out on the radial plot in Figure 4. For instance, in Port
22 Sudan, Sheffield and Bandung, significant reductions in affected population are projected to be 100% due to
23 climate change, however large projected increases (~300 to 400%) in damages are due mostly to development.
24 In Leshan, development is projected to slightly lower the amount of affected population and also to increase
25 damages costs more than three-fold.

1 24: 'Asia'). However, socioeconomic growth in this area is projected to have even more of an impact on urban
2 floods than climate change is. Flood risk and human and material losses are already heavily concentrated in India,
3 Bangladesh and China (Pachauri et al., (2014), chapter 24: 'Asia'), and Jongman (2012) estimates the largest
4 current and future economic exposure to river floods to be in Asia. As an example, we take a closer look at Dhaka
5 which, with a GDP per capita of \$1212 in 2015, already has one of the highest levels of population affected annually
6 by flooding (over 130,000) and this number is projected to increase almost five-fold to over 630,000 by 2030.
7 The greatest change predicted for Dhaka, though, is an almost 22-fold increase in annual damage costs (from \$8
8 million to \$175 million). Dhaka is subjected to regular flooding from surrounding rivers, with peak flows in the
9 Brahmaputra and Ganges Rivers coinciding to exacerbate flood impacts. In the past, most low-lying areas of
10 western Dhaka were infilled for residential and commercial use, causing a reduction in areas for flood water
11 storage. Furthermore, uncontrolled and unplanned urban expansion is spreading rapidly across the floodplains
12 in the east of the city placing more people in flood hazard zones (Kreimer et al., 2003). These hasty
13 developmental changes are having more of an impact on the urban hydrology of Dhaka than the climate change
14 is. Other examples of cities in similar situations include Kolkata (with the highest baseline affected population in
15 this study), Mumbai (with a seven-fold increase in both population affected and damages due 40% and 60%,
16 respectively, to development), Bangkok (with large increases 50-75% of which are attributed to development)
17 and Ho Chi Minh City (with a 50% increase in affected population and an over five-fold increase in damages costs,
18 almost entirely attributed to development).

19 Globally, migration trends are seeing more people moving into informal settlements in urban flood zones – the
20 population exposed to river flooding increased by 2.6% more than total global population growth between 1970
21 and 2010 (Jongman et al., 2012). Most global population growth in the near future is projected to occur in cities
22 of lower income countries, organically and through migration (Kreimer et al., 2003), with urban populations in
23 these countries growing at a rate five times faster than in higher income countries (UN-DESA, 2015) and predicted
24 to double in the next 30 years (Angel et al., 2010). The same regions experiencing such high urban population
25 growth are also projected to triple their urban footprint in the same timeframe (Angel et al., 2010). These
26 developmental changes are leading to, and will continue to produce, substantial effects on urban hydrology if
27 not countered.

28 Developmental changes in some cities, however, appear to be effectively reducing impacts from river flooding.
29 Marrakech, in cluster 15, is an example of this. The affected population level is projected to decrease mostly due
30 to socioeconomic factors (website 3; Ward et al., 2013; Winsemius et al., 2013). Morocco is taking responsibility
31 to make efforts countering global climate change, and through an 'Integrated Disaster Risk Management and
32 Resilience Program for Morocco' (World Bank, April 2016-Dec 2021), is making its population more resilient to
33 climate change, less vulnerable to natural hazards and ensuring a rapid transition to a low-carbon economy.
34 Through Morocco's National Strategy for Sustainable Development, a commitment has been made to reduce
35 national greenhouse gas emissions by 32% by 2030, through an increase in renewable energy sources to 50% by
36 2025, a reduction in energy consumption by 15% by 2030, as well as various agricultural, water, waste, forest,
37 industry and housing initiatives (website 9). These housing initiatives in Marrakech include a slum clearance and
38 relocation project, which has become part of urban policy (Ibrahim, 2016), reducing the amount of people
39 inhabiting flood hazard zones. Alert systems in the valleys of the Atlas region above Marrakech have been
40 improved, and the proportion of the population living in slums has decreased from over 8% in 2004 to less than
41 4% in 2010 (UN-Habitat website). The urbanization rate in Morocco is also projected to slow down towards 2030
42 (UN-Habitat website). This risk-prevention approach combining early warning systems, relocation of inhabitants
43 out of the flood zone, and less urban expansion is expected to combine to reduce the impact of floods on the
44 population of Marrakesh.

1 The analysis in this paper is based solely on the data provided in Aqueduct, regardless of the extent to which on-
2 the-ground flood management measures are incorporated into the socioeconomic models which produced this
3 data. A discussion characterizing individual cities is included here as a point of interest to relate the data to
4 current national conditions, providing possible reasons why these cities may fit into the map where they do.

5 Current high flood impact conditions projected to get much greater primarily due to climate change are
6 anticipated for cities in the lower right of SOM3, with high magnitude changes expected for impacts on both
7 population and property. One of these cities, Sao Paulo, for instance, is expected to experience an almost seven-
8 fold increase in both the number of population affected (to over 140,000 annually) and urban damages costs (to
9 over \$500,000,000 annually) by 2030. 15% of the change in population and 35% of the change in damages is
10 attributed to development, but the majority of the change is projected to be caused by climate change. Sao
11 Paulo is the largest city in Brazil, and the city footprint is projected to increase over 38% by 2030, by which time
12 22% of the urban area may be located in flood zones (Young, 2013). The IPCC (Pachauri et al., (2014) chapter 14
13 'Latin America') predicts the increase in temperature in central and south Brazil to be the largest projected
14 increase in Latin America, which will be combined with a +10 to +15% increase in autumn precipitation, greatly
15 affecting the hydrologic cycle in the region. The substantial change in development is therefore expected to be
16 eclipsed by the even greater projected change in climate in Sao Paulo.

17 The anticipated reduction in flood damage costs caused by climate change (evident in Cluster 15) may be a result
18 of changing snow melt conditions upstream of these cities. It has been shown that some global regions will
19 experience a decreasing trend in the magnitude and frequency of snow melt floods as the climate warms, as
20 well as a shift in the timing of these floods (Schiermeier, 2011; Barnett et al., 2005; Immerzeel et al., 2010).
21 Although changing climate in some areas is projected to lessen regional flooding, development within urban
22 flood zones may be severe enough to offset any reductions in flood impacts. This can be seen most prominently
23 in a strip on the left of SOM3 stretching from Port Sudan down to Santiago.

24 Many high-income cities with already high current flood vulnerabilities have projections for large elevations in
25 damage costs, but not increased levels of affected population. This can be seen in cities on SOM3 centred around
26 London, Tokyo, LA and Vienna (cluster 3), and Sydney and Castellon (cluster 13). Through high levels of planning,
27 preparedness and infrastructure, prosperous regions generally have systems in place to minimize flood impacts
28 on the population, even though they may incur large economic losses (Desai et al., 2015; Kreimer et al., 2003).
29 Almost half of the projected increases in these clusters are attributed to development, suggesting that these
30 cities may have the capacity for lessening potentially elevated flood damage costs by concentrating on planning
31 and mitigation policies.

32 Though this study does not consider coastal flooding, it may be noted that due to their locations near river
33 mouths, many of the cities in the lower left of the map that are projected to experience high increases in impacts
34 from river flooding are also at risk of increased coastal flooding from intensified storms and sea level rise due to
35 climate change. Mumbai, Guangzhou, Shanghai, Ho Chi Minh City, Kolkata, Bangkok, and Dhaka are 7 of the top
36 14 cities (out of 136) ranked by current population exposure to coastal flooding. These same cities also comprise
37 the top 7 cities (in this order: Kolkata, Dhaka, Mumbai, Guangzhou, Ho Chi Minh City, Shanghai, Bangkok) ranked
38 by future (2070) estimated population exposed to coastal flooding (UNEP, 2016; Nicholls et al., 2008).

39 Almost all projected changes in flooding in this data set are of a relatively similar order of magnitude to the
40 original effects, as can be observed on Figure 4. That is, most cities that are only marginally affected by flooding
41 in 2010 are projected to experience only small increases by 2030, whereas cities with larger flood effects can
42 expect greater changes. A significant correlation exists between the magnitudes of the cities' baseline flooding

1 effects and the changes projected by 2030 (log-transformed absolute values for both variables) – an 88%
2 correlation exists in the number of population affected and a 94% correlation for property damage costs. This
3 supports the findings of Milly et al. (2002) who observed that the frequency of large flood events in large basins
4 had increased substantially in the 20th century, but smaller floods had not.

5 5 CONCLUSION

6 Global patterns of urban flood responses to global and local changes in hydrology driven by climate change and
7 development have been identified and visually communicated. Cities have been matched to these global
8 patterns, and relationships between the individual cities have been discerned with respect to baseline flooding
9 conditions and expected future changes. Information has been extracted from a large, recently released, global
10 data set of city-level flood impacts relating hydrology and urban development, and combined with city-specific
11 demographic information. The analysis and visual interpretation in this study has revealed interesting city-level
12 patterns that are otherwise unobservable in the complex data set, and provides a comparison and distinction
13 between individual cities that is not apparent in regional- or economic-level projections.

14 We have performed dimension reduction and clustering with a series of self-organizing maps to identify
15 changing global patterns of city-level flood risks. The maps provide an indication of the predominant
16 characteristics which determine the differences in urban river flood impacts between cities, and the cities occupy
17 positions on the maps signifying their relative conditions. The method used here incorporates adaptations to the
18 self-organising map technique for map shape selection and temporal pattern extraction, allowing two levels of
19 information to emerge: the characteristic patterns of dynamic global urban flood vulnerabilities, and a
20 comparison between the cities with respect to flood characteristics and trends.

21 A shortcoming of the method used here is the assignment of flood protection level based on an assumption of
22 proportionality with national income level. As standardised, current information on the real flood protection
23 levels of all the cities in the data set is not readily available, this assumption has been necessary and has been
24 made in line with current practice. This limitation has been recently acknowledged in the literature, with
25 Winsemius et al. (2016) noting that ‘currently installed flood protection is an important missing link in the
26 assessment of global flood risk’. Future studies may aim to include specific flood protection levels for each city.

27 Whilst the timeline of this study is short, it is restricted by the data that is available. Studies at a global scale have
28 been traditionally limited due to lack of cohesive data sets, and therefore the data set provided by Aqueduct is
29 valuable for the fact that it spans a global set of cities and provides a rare opportunity for comparison. As the
30 data is only provided for 2010 and 2030, there was no prospect for a longer analysis. Whilst this analysis may not
31 provide a long-term outlook, at the very least an important insight into the current and near-future conditions
32 can be gained.

33 Cities have major implications for climate change mitigation and adaptation (Revi et al., 2014). Unplanned
34 development and urban migration are increasing vulnerabilities to natural hazards (UNEP, 2016) and land cover
35 change and greenhouse gas emissions are intensifying urban hydrology. Understanding the relationship
36 between flood impacts and social vulnerability is a necessary step for prioritizing flood mitigation and prevention
37 strategies (Doocy et al., 2013). Whether the main driver of increased urban flood impacts is development or
38 climate change, cities will benefit from development restrictions and planning standards for urban expansion,
39 sustainable land development, management of population distribution and migration, and early warning
40 systems and preparedness (Revi et al., 2014; UN-DESA, 2014; Doocy et al., 2013).

1 This study adds to the understanding of natural hazards in a global context, which is an important aspect of
2 regional disaster risk management due to the dependency of local situations on global processes (Desai et al.,
3 2015). The complex nonlinear socio-environmental relationships make it difficult to foresee local responses to
4 global changes (Desai et al., 2015), and therefore this study focuses on risk communication (the process between
5 risk perception and adaptation planning (Cardona et al., 2012)) to provide a visual analysis of the global patterns
6 of evolving flood impacts, socioeconomic development and climate change, and the local city-level
7 consequences of these changes.

8 Future work may include the addition of greenhouse gas emissions data, geographic location, city sizes and
9 densities to this study, to discern the relationships of these factors with urban flood changes. Greenhouse gas
10 emissions are the largest contributor to global warming, leading to alterations in the intensity of the hydrologic
11 cycle (Pachauri et al., 2014, Barnett et al., 2005; Wentz et al., 2007; Schiermeier, 2011), and cities are the major
12 contributors of greenhouse gases, with a large proportion of global emissions produced by a small global land
13 area (Mills, 2007; Angel et al., 2010; Revi et al., 2014). The addition of these elements could highlight the essential
14 role cities could play in climate change mitigation and the reduction of urban flood impacts.

6 REFERENCES

- 1
2 Agarwal, P, and Skupin, A. (2008). *Self-organising maps: Applications in geographic information science*, John
3 Wiley & Sons.
- 4 Angel, S, Parent, J, Civco, D, & Blei, A. (2010a). *Atlas of Urban Expansion*, Cambridge MA: Lincoln Institute of Land
5 Policy.
- 6 Angel, S, Parent, J, Civco, D, Blei, A, & Potere, D. (2010b). *A Planet of Cities: Urban Land Cover Estimates and
7 Projections for All Countries, 2000-2050*. Lincoln Institute of Land Policy Working Paper.
- 8 Barnett, T, Adam, J & Lettenmaier, D. (2005). Potential impacts of a warming climate on water availability in
9 snow-dominated regions. *Nature*, 438(7066), 303-309.
- 10 Clark, S, Sarlin, P, Sharma, A, & Sisson, SA. (2015). Increasing dependence on foreign water resources? An
11 assessment of trends in global virtual water flows using a self-organizing time map. *Ecological Informatics*, 26,
12 192-202.
- 13 Clark, S, Sisson, SA, & Sharma, A. (2016). A dimension range representation (DRR) measure for self-organizing
14 maps. *Pattern Recognition*, 53, 276-286.
- 15 Clark, S, Sisson, SA, & Sharma, A. (2016b, in press). Nonlinear manifold representation in natural systems.
16 *Environmental Modelling and Software*.
- 17 Cunderlik, JM, & Ouarda, T. (2009). Trends in the timing and magnitude of floods in Canada. *Journal of Hydrology*,
18 375(3), 471-480.
- 19 Davies, DL, & Bouldin, DW. (1979). A cluster separation measure. *Pattern Analysis and Machine Intelligence, IEEE
20 Transactions (2)*, 224-227.
- 21 Desai, B, Maskrey, A, Peduzzi, P, De Bono, A, & Herold, C. (2015). *Making Development Sustainable: The Future
22 of Disaster Risk Management, Global Assessment Report on Disaster Risk Reduction*. Geneva, Switzerland:
23 United Nations Office for Disaster Risk Reduction.
- 24 Doocy, S, Daniels, A, Murray, S, & Kirsch, TD. The human impact of floods: A historical review of events 1980–
25 2009 and systematic literature review. *PLoS Curr*, 16, 12.
- 26 Frich, P, Alexander, LV, Della-Marta, P, Gleason, B, Haylock, M, Tank, A, & Peterson, T. (2002). Observed coherent
27 changes in climatic extremes during the second half of the twentieth century. *Climate Research*, 19(3), 193-212.
- 28 Ibrahim. (2016). *Slum eradication policies in Marrakech, Morocco*. World Bank Conference on Land and Poverty,
29 Washington DC.
- 30 Immerzeel, WW, Van Beek, LPH, & Bierkens, MFP. (2010). Climate change will affect the Asian water towers.
31 *Science*, 328(5984), 1382-1385.
- 32 Jiang, L, & O'Neill, BC. (2015). Global urbanization projections for the Shared Socioeconomic Pathways. *Global
33 Environmental Change*.
- 34 Jongman, B, Ward, PJ, & Aerts, JC. (2012). Global exposure to river and coastal flooding: Long term trends and
35 changes. *Global Environmental Change*, 22(4), 823-835.
- 36 Jongman B, Winsemius HC, Aerts JC, de Perez, EC, van Aalst, MK, Kron, W, Ward, PJ. (2015) Declining vulnerability
37 to river floods and the global benefits of adaptation. *Proceedings of the National Academy of Sciences*. May
38 5 ;112 (18): E2271-80.
- 39 Kaski, S, & Kohonen, T. (1996). Exploratory data analysis by the self-organizing map: Structures of welfare and
40 poverty in the world. *Proceedings of the third international conference on Neural Networks in the Capital
41 Markets*.
- 42 Katz, RW, Parlange, MB, & Naveau, P. (2002). Statistics of extremes in hydrology. *Advances in water resources*,
43 25(8), 1287-1304.

1 Kiviluoto, K. (1996). Topology preservation in self-organizing maps. IEEE International Conference on Neural
2 Networks.

3 Kohonen, T. (2001). Self-organizing maps, Volume 30 of Series in Information Sciences.

4 Kreimer, A, Arnold, M, & Carlin, A. (2003). Building safer cities: the future of disaster risk: World Bank Publications.

5 Kumm, M, De Moel, H, Ward, PJ, & Varis, O. (2011). How close do we live to water? A global analysis of population
6 distance to freshwater bodies. PLoS One, 6(6), e20578.

7 Kunkel, KE, Pielke Jr, Roger A, & Changnon, SA. (1999). Temporal fluctuations in weather and climate extremes
8 that cause economic and human health impacts: A review. Bulletin of the American Meteorological Society,
9 80(6), 1077.

10 Meehl, GA, Arblaster, JM, & Tebaldi, C. (2005). Understanding future patterns of increased precipitation intensity
11 in climate model simulations. Geophysical Research Letters, 32(18).

12 Mills, G. (2007). Cities as agents of global change. International Journal of Climatology, 27(14), 1849-1857.

13 Milly, PCD, Dunne, KA, & Vecchia, AV. (2005). Global pattern of trends in streamflow and water availability in a
14 changing climate. Nature, 438(7066), 347-350.

15 Milly, PD, Wetherald, RT, Dunne, KA, & Delworth, TL. (2002). Increasing risk of great floods in a changing climate.
16 Nature, 415(6871), 514-517.

17 Muis, S, Güneralp, B, Jongman, B, Aerts, JC, Ward, PJ. (2015) Flood risk and adaptation strategies under climate
18 change and urban expansion: A probabilistic analysis using global data. Science of the Total Environment. 538:
19 445-57.

20 Nature. (2016). Waters encroaching. Nature Climate Change, 6(7), 635, editorial.

21 Nicholls, RJ, Hanson, S, Herweijer, C, Patmore, N, Hallegatte, S, Corfee-Morlot, J, Muir-Wood, R. (2008). Ranking
22 port cities with high exposure and vulnerability to climate extremes.

23 Pachauri, RK, Allen, MR, Barros, VR, Broome, J, Cramer, W, Christ, R, ... & Dubash, NK. (2014). Climate Change
24 2014: Synthesis Report. Contribution of Working Groups I, II and III to the Fifth Assessment Report of the
25 Intergovernmental Panel on Climate Change (p. 151). IPCC.

26 Revi, A, Satterthwaite, DE, Aragón-Durand, F, Corfee-Morlot, J, Kiunsi, RBR, Pelling, M, Roberts, DC & Solecki, W.
27 (2014). Urban areas. In: Climate Change 2014: Impacts, Adaptation, and Vulnerability. Part A: Global and Sectoral
28 Aspects. Contribution of Working Group II to the Fifth Assessment Report of the Intergovernmental Panel on
29 Climate Change. United Kingdom and New York, NY, USA: Cambridge University Press, Cambridge.

30 Samir, KC, & Lutz, W. (2014). The human core of the shared socioeconomic pathways: Population scenarios by
31 age, sex and level of education for all countries to 2100. Global Environmental Change.

32 Schiermeier, Q. (2011). Increased flood risk linked to global warming. Nature, 470(7334), 316.

33 Shanmuganathan, S, Sallis, P, & Buckeridge, J. (2006). Self-organising map methods in integrated modelling of
34 environmental and economic systems. Environmental Modelling & Software, 21(9), 1247-1256. doi:
35 10.1016/j.envsoft.2005.04.011.

36 Sheppard, SRJ. (2005). Landscape visualisation and climate change: the potential for influencing perceptions and
37 behaviour. Environmental Science & Policy, 8(6), 637-654.

38 Skupin, A, & Hagelman, R. (2005). Visualizing demographic trajectories with self-organizing maps.
39 Geoinformatica, 9(2), 159-179.

40 Sofia, G, Roder, G, Dalla, FG, Tarolli, P. (2017) Flood dynamics in urbanised landscapes: 100 years of climate and
41 humans' interaction. Scientific reports.

42 Ultsch, A. (2003). U-matrix: a tool to visualize clusters in high dimensional data. Marburg: Fachbereich
43 Mathematik und Informatik.

- 1 UN-DESA. (2015). World Urbanization Prospects: The 2014 Revision. New York: United Nations Department of
2 Economic and Social Affairs.
- 3 UNEP. (2016). Summary of the sixth global environment outlook regional assessments: Key findings and policy
4 messages. United Nations Environment Programme.
- 5 UN-Habitat. (2010). State of the world's cities. Earthscan.
- 6 UN-Habitat. (2014). Urban Equity in Development - Cities for Life. World Urban Forum 7. April 2014, Medellin,
7 Colombia.
- 8 Václavík, T, Lautenbach, S, Kuemmerle, T, & Seppelt, R. (2013). Mapping global land system archetypes. *Global
9 Environmental Change*, 23(6), 1637-1647.
- 10 Vesanto, J, & Alhoniemi, E. (2000). Clustering of the self-organizing map. *IEEE Transactions on Neural Networks*,
11 11(3), 586-600. doi: 10.1109/72.846731.
- 12 Ward, JHJr. (1963). Hierarchical grouping to optimize an objective function. *Journal of the American Statistical
13 Association*, 58, 236-244.
- 14 Ward, PJ, Jongman, B, Weiland, FS, Bouwman, A, van Beek, R, Bierkens, MF, ... & Winsemius, HC (2013). Assessing
15 flood risk at the global scale: model setup, results, and sensitivity. *Environmental research letters*, 8(4), 044019.
- 16 Wasko, C, & Sharma, A. (2015). Steeper temporal distribution of rain intensity at higher temperatures within
17 Australian storms. *Nature Geoscience* 8.7: 527-529.
- 18 Wentz, FJ, Ricciardulli, L, Hilburn, K, & Mears, C. (2007). How much more rain will global warming bring? *Science*,
19 317(5835), 233-235.
- 20 Willems, P, Olsson, J, Arnbjerg-Nielsen, K, Beecham, S, Pathirana, A, Gregersen, IB, & Madsen, H. (Eds.).
21 (2012). Impacts of climate change on rainfall extremes and urban drainage systems. IWA publishing.
- 22 Winsemius, HC, Van Beek, LPH, Jongman, B, Ward, PJ, & Bouwman, A. (2013). A framework for global river flood
23 risk assessments. *Hydrology and Earth System Sciences*, 17(5), 1871-1892.
- 24 Winsemius, HC, Aerts, JC, van Beek, LP, Bierkens, MF, Bouwman, A, Jongman, B, Kwadijk, JC, Ligtoet, W, Lucas,
25 PL, van Vuuren, DP, Ward, PJ. (2016) Global drivers of future river flood risk. *Nature Climate Change*, 6(4): 381-5.
- 26 Young, AF. (2013). Urban expansion and environmental risk in the São Paulo Metropolitan Area. *Climate Research*,
27 57(1), 73-80.

28
29

Websites:

- 30 1. **Atlas of Urban Expansion:** [http://www.lincolnst.edu/subcenters/atlas-urban-](http://www.lincolnst.edu/subcenters/atlas-urban-expansion/Default.aspx)
31 [expansion/Default.aspx](http://www.lincolnst.edu/subcenters/atlas-urban-expansion/Default.aspx)
- 32 2. **World Bank's World Development Indicators database:** [http://data.worldbank.org/data-](http://data.worldbank.org/data-catalog/world-development-indicators)
33 [catalog/world-development-indicators](http://data.worldbank.org/data-catalog/world-development-indicators)
- 34 3. **World Resources Institute's Aqueduct Global Flood Analyzer Tool:** <http://floods.wri.org/#/>
- 35 4. **ISIMIP:** [https://www.pik-potsdam.de/research/climate-impacts-and-vulnerabilities/research/rd2-](https://www.pik-potsdam.de/research/climate-impacts-and-vulnerabilities/research/rd2-cross-cutting-activities/isi-mip/about)
36 [cross-cutting-activities/isi-mip/about](https://www.pik-potsdam.de/research/climate-impacts-and-vulnerabilities/research/rd2-cross-cutting-activities/isi-mip/about)
- 37 5. **Shared Socioeconomic Pathways:**
38 <https://tntcat.iiasa.ac.at/SspDb/dsd?Action=htmlpage&page=about>
- 39 6. **World Resources Institute's Aqueduct Global Flood Risk Country Rankings:**
40 <http://www.wri.org/resources/data-sets/aqueduct-global-flood-risk-country-rankings>
- 41 7. **SOM Toolbox:** <http://www.cis.hut.fi/somtoolbox>
- 42 8. Scientific American: [https://www.scientificamerican.com/article/extreme-rain-may-flood-54-million-](https://www.scientificamerican.com/article/extreme-rain-may-flood-54-million-people-by-2030/)
43 [people-by-2030/](https://www.scientificamerican.com/article/extreme-rain-may-flood-54-million-people-by-2030/)

1 9. **United Nations Framework Convention on Climate Change:** www4.unfccc.in

2 **7 COMPETING INTERESTS**

3 The authors declare that they have no conflicts of interest

